Article

Not peer-reviewed version

Enhanced Energy Harvesting from Thermoelectric Modules: Strategic Manipulation of Element Quantity and Geometry for Optimized Power Output

Chun-I Wu *, Kung-Wen Du, Yu-Hsuan Tu

Posted Date: 23 September 2024

doi: 10.20944/preprints202409.1792.v1

Keywords: Thermoelectric generators; Annular thermoelectric generators; Waste heat recovery; Energy harvesting; Module design and optimization; Energy conversion efficiency; Thermocouple optimization

Article

Enhanced Energy Harvesting from Thermoelectric Modules: Strategic Manipulation of Element Quantity and Geometry for Optimized Power Output

Chun-I Wu [1,*,†], Kung-Wen Du [1,†] and Yu-Hsuan Tu [2]

[1] Department of Mechanical and Mechatronic Engineering, National Taiwan Ocean University, Keelung 20224, Taiwan
[2] Department of Green Energy and Information Technology, National Taitung University, Taitung 95092, Taiwan
* Correspondence: wuchuni@ntou.edu.tw; Tel.: +886-938-706-502
† Co-first author, these authors contributed equally to this paper.

Abstract: With the rising awareness of environmental issues, concerns about pollution and global warming have gained importance, and electricity generation costs continue to increase. As a result, research on energy recovery using thermoelectric modules has attracted attention in recent years. Given the lack of significant breakthroughs in thermoelectric materials, improving the structure of thermoelectric modules has become a key direction for enhancing efficiency. Common thermoelectric module types include flat plate (Flat Plate TEG), annular (Annular TEG), flexible (Flexibility TEG), segmented, and cascaded designs. Factors influencing thermoelectric performance include the number, shape, height, contact area of thermoelectric elements, temperature difference, copper plate length, contact resistance, and the geometric arrangement of the elements. This study is based on the commercially available TGM1-127-1.0-0.8 thermoelectric module. By simulating the output performance of both flat plate and annular thermoelectric module structures under identical conditions—such as total volume of thermoelectric material, shape, and height of the thermoelectric legs, the total contact area with the heat source, temperature differential, and total volume of the connecting copper plate—we observed that the number of thermoelectric elements not only determines the open-circuit voltage but also influences the output power. The trend of output power remains consistent under varying temperature differences, regardless of changes in the load resistance.

Keywords: thermoelectric generators; annular thermoelectric generators; waste heat recovery; energy harvesting; module design and optimization; energy conversion efficiency; thermocouple optimization

1. Introduction

Energy loss occurs during the energy conversion process due to low conversion efficiency. For example, in an internal combustion engine, only about 1/3 of the fuel can be converted into electrical energy [1]. In the United States, approximately 33% of industrial waste energy is heat, potentially equal to 0.9 to 2.8 TWh of electricity annually [2]. Thermoelectric materials, which can convert waste heat into energy directly, have attracted significant attention [3].

Thermoelectric generators (TEGs) offer direct energy conversion, operate without moving parts, require minimal maintenance, occupy little space, and are ideal for embedded systems due to their noise-free operation, making them highly suitable for waste heat recovery [4]. Recent discussions have focused on optimizing the geometry and structure of thermoelectric modules, which significantly enhances their performance. This includes thermoelectric elements' height, cross-sectional area, number, and shape [5]. Thus, the physical design of a TEG is a crucial factor in its efficiency.

Several studies have explored the impact of these variables. For instance, Shouyuan Huang and Xianfan Xu emphasized the need for structural design and computational analysis to improve output power, thermal efficiency, and reliability while balancing these parameters [6]. Yohann Thimont and colleagues analyzed 16 thermoelectric units, revealing the substantial effect of leg geometry on

 doi:10.20944/preprints202409.1792.v

thermal resistance and output power [7]. Rapid engineering advancements have enabled the flexible design of thermoelectric materials in various geometric shapes[8–10].

Many studies have been interested in annular thermoelectric generators (ATEGs) [9,11]. WenChao Zhu and others highlighted that ATEGs exhibit higher energy conversion efficiency than flat-plate models and used advanced genetic algorithms to optimize ATEG performance[12].

When considering optimizing component sizes within thermoelectric modules, most studies primarily focus on the losses due to contact resistance of the thermoelectric elements[13,14] and internal thermal transfer losses [15]. Researchers such as A. Narjis et al. [16] and F.P. Brito et al. [17] found that thermal resistance between the thermoelectric elements and the heat source is one of the main factors affecting output power. Tingzhen Ming and colleagues [18] improved output power by 3.89% to 5.33% through optimized combinations and rearrangements of P-type and N-type thermoelectric elements. Lei Wang and others [19] analyzed factors such as the thickness of the thermoelectric elements, cross-sectional areas of P-type and N-type elements, insulating materials, and the thickness of the connecting copper strips, discovering that specific thicknesses of the copper strips could maximize the output power of the thermoelectric module.

Shifa Fan and Yuanwen Gao [20] observed that increasing the height of the thermoelectric elements in ATEGs could enhance their mechanical performance, albeit at the cost of reduced power output. However, increasing the angle of annular thermoelectric elements at a fixed height could increase the output power without compromising their mechanical performance. Mengjun Zhang and colleagues [21] compared the distribution of heat sources and output power within annular and flat-plate heat exchangers under the same area of heat exposure and heat exchanger inlet conditions for thermoelectric elements.

The quantity of thermocouples significantly impacts the performance of thermoelectric modules, as found by Jun Wang et al. [22] in simulation experiments where open-circuit voltage and output power were directly proportional to the number of thermocouples. While increasing the number of thermocouples in series within a heat exchanger also increases the heat-receiving area, thereby increasing the open-circuit voltage [23], Mohamed M. Elsabahy et al. [24] noted that the output power of thermoelectric modules primarily depends on physical characteristics, dimensions, configuration, number of thermocouples, and other parameters. Therefore, changing the shape of thermoelectric elements without altering their volume, height, or cross-sectional area could lead to a study on output performance. Fankai Meng and others [25] optimized the internal physical dimensions (the length and the cross-sectional area of the thermocouples) to enhance performance through stability analysis, including parameters like steady current, heating load, performance coefficient, maximum heating load, and maximum temperature difference. Linhao Fan, Pan Wang, and colleagues [26,27] used thermoelectric materials of the same volume to simulate different ratios of lengths and heated areas for rectangular and cylindrical thermoelectric elements, calculating optimal ratios and thermoelectric output performance. Matthew M. Barry and others [28] combined rectangular thermoelectric elements with temperature-dependent material properties and independent thermal and electrical contact resistances; optimizing their geometric shape in terms of cross-sectional area and length could produce maximum thermal conversion efficiency or maximum power output. Yongming Shi et al. [29] noted that many computational studies on thermocouples have been conducted, but most are based on unchanged geometrical shapes and numbers of thermocouples. As mentioned earlier, it is evident from the literature that the established research methods and numerical analysis models significantly aid in increasing the output power of a single thermoelectric element.

This research aims to maintain the overall size of the thermoelectric module while simulating variations in the shape, height, and total contact area of the heat source, keeping the volume of the connecting copper plate constant. By observing the performance changes in annular and flat-plate thermoelectric generators with different numbers of thermoelectric elements, we aim to offer insights into optimizing thermoelectric module performance.

 doi:10.20944/preprints202409.1792.v

2. Model

2.1. Module 1

The flat-plate thermoelectric generator (FTEG), a commonly commercialized thermoelectric module in the market, is the focus of this study. The research uses the specifications and material qualities of the TGM1-127-1.0-0.8 thermoelectric module manufactured by KRYOTHERM in Saint Petersburg, Russia. These details may be found in Reference [29] and are presented in Table 1. This specific thermoelectric module consists of 127 internal thermocouple pairs. The dimensions of each thermoelectric element are 1(L) x 1(W) x 1.35(H) mm. The conductive metal utilized for interconnecting these thermoelectric elements possesses dimensions of 2.5(L) x 1(W) x 0.1(H) mm. The distance between each thermoelectric element is 0.5 mm. The combined surface area of contact between the thermoelectric devices within the module and the heat source is 254 mm^2. The flat-plate thermoelectric module is equipped with ceramic layers that have dimensions of 23.5(L) x 23.5(W) x 0.1(H) mm. These layers are placed both at the top and bottom of the module. The ceramic layers secure and safeguard the thermoelectric elements while providing insulation from the materials at the cold and hot ends. Figures 1 and 2 depict the measurements of the FTEG and its internal thermocouples.

Table 1.

Effective Material Properties		
α[1]=314.96 μ • V/K	k[2]=0.03 W/cm • K	ρ[3]=2.23*10-3 Ω • cm

[1] α is Seebeck coefficient, [2] k is thermal conductivity, [3] ρ is resistivity.

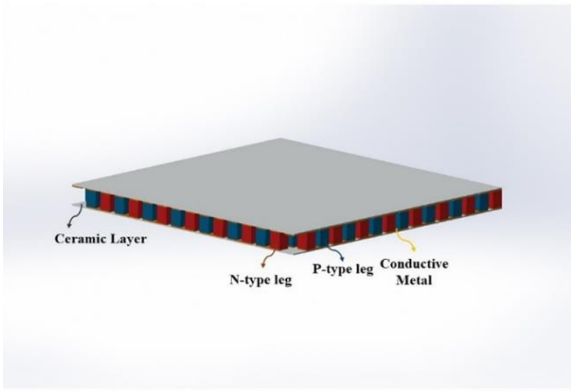

Figure 1. TGM1-127-1.0-0.8 Thermoelectric Module Illustration – a detailed view of the module used in the experiments, highlighting its key components and specifications.[30].

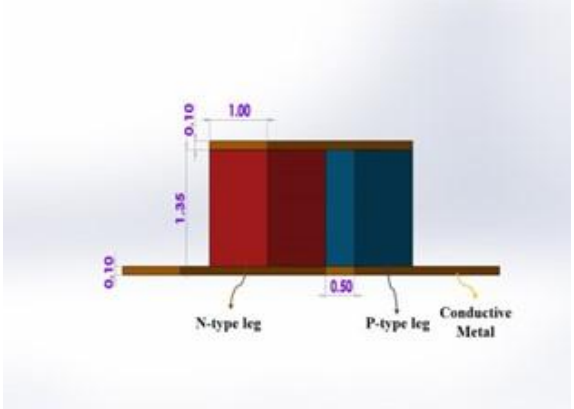

Figure 2. TGM1-127-1.0-0.8 Thermocouple Pair – an illustration of the thermocouple pair configuration within the TGM1-127-1.0-0.8 module, detailing the arrangement and key features.[30].

 doi:10.20944/preprints202409.1792.v

2.2. Module 2: Traditional Annular Thermoelectric Generator

ATEG comprises numerous annular thermoelectric elements arranged in an arc formation, interconnected by arc-shaped conductive metal plates, as illustrated in Figure 3. Based on the ATEG structure data proposed by Xiao-Xiao Tian et al. [31], we simulated an ATEG with the same thermoelectric material volume as the TGM1-127-1.0-0.8 thermoelectric module. This ATEG consists of 108 thermocouple pairs, with each annulus holding 12 thermocouple pairs. Each thermoelectric element is inclined at 10°, with a 5° angle between two neighboring components. The inclination of each thermocouple pair is 25°. The thermoelectric element has an external radius of 9.19 mm and an internal radius of 8.15 mm. It has a height of 1.05 mm and a width of 1 mm. The combined surface area of contact between the thermoelectric devices and the heat source measures 306.87 mm². The height (H) of the connecting copper strips is 0.1 mm. The ATEG module is coated with ceramic layers, each with a thickness of 0.1 mm, on both its inner and outer sides. The purpose of these ceramic layers is to ensure stability and safeguard the thermoelectric elements housed within the module.

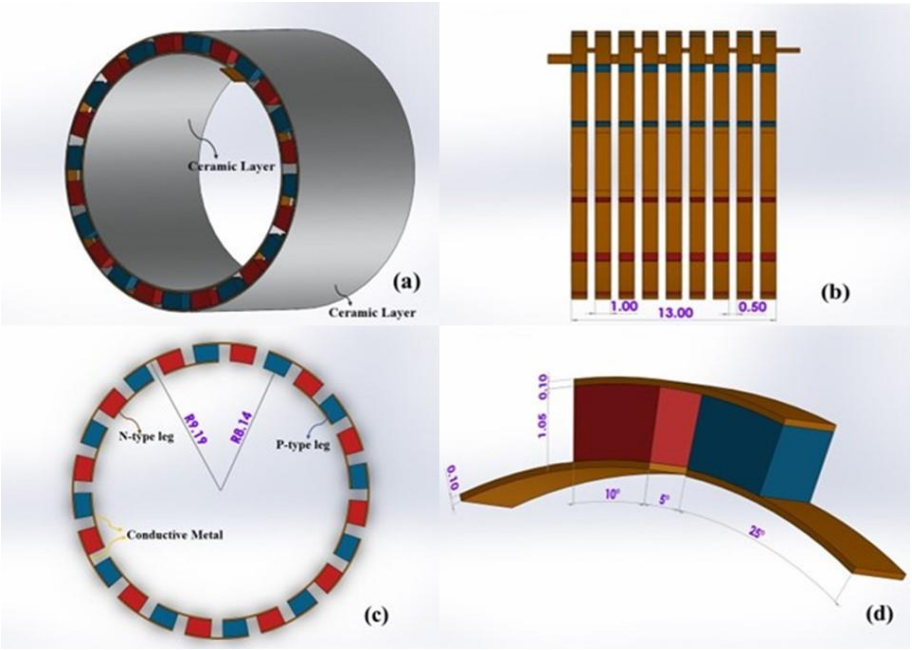

Figure 3. ATEG Structural Diagrams – (a) Overview of the Annular Thermoelectric Generator (ATEG), (b) Side View of ATEG, (c) Single Ring Structure of ATEG, (d) Dimensional Diagram of Thermoelectric Elements.[30].

2.3. Module 3 Focuses on the Validation Model for Annular Thermoelectric Generator

In order to assess the influence of the number of thermoelectric elements on the generated power of ATEG, our simulations are conducted using the specific number and dimensions of thermocouples illustrated in Figure 3 (c)(d). Following that, we constructed two more variations of ATEGs, each with a distinct quantity of single-ring thermocouples: one with 24 pairs (depicted in Figure 4) and another with six pairs (depicted in Figure 5). Hence, the validation process involved the utilization of three single-ring ATEGs, each equipped with 24, 12, and 6 thermocouple pairs, respectively. Despite differences in the number of thermocouples, these three single-ring ATEGs have the same total volumes of thermoelectric material, identical dimensions for each thermoelectric element, the same contact area with the heat source, and the same volume of conductive metal used. We evaluate the impact of the different quantities of thermoelectric elements on the output power by comparing these three thermoelectric modules.

 doi:10.20944/preprints202409.1792.v

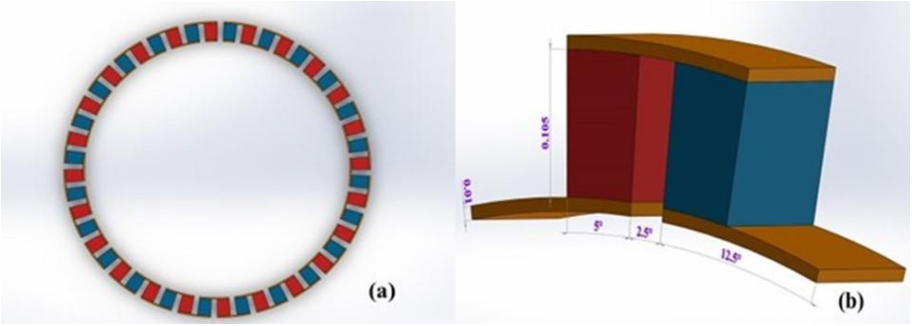

Figure 4. Annular Thermoelectric Generator with 24 Thermocouple Pairs – (a) Single Ring Structure of ATEG, (b) Dimensional Diagram of Thermoelectric Elements. [30].

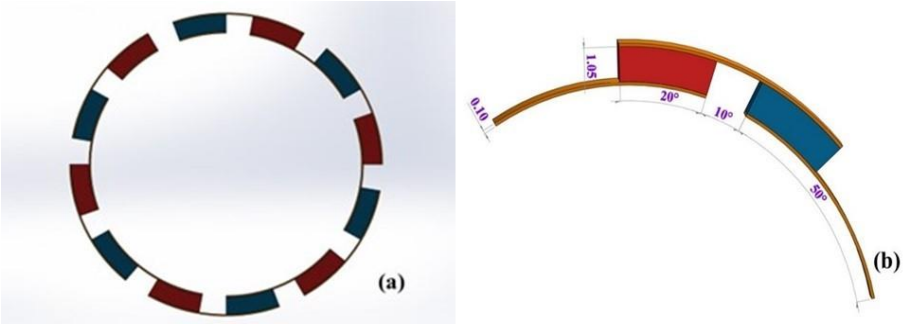

Figure 5. Annular Thermoelectric Generator with 6 Thermocouple Pairs – (a) Single Ring Structure of ATEG, (b) Dimensional Diagram of Thermoelectric Elements.[30].

2.4. Module 4: Validation Model for Flat-Plate Thermoelectric Generator

In order to assess the influence of the number of thermoelectric elements in an FTEG on its power output, we utilize the number of thermocouples present in a solitary row of the TGM1-127-1.0-0.8 thermoelectric module, as depicted in fig.6(a), as a reference point. Following that, we proceed to replicate and construct supplementary thermoelectric modules that possess identical characteristics in terms of the overall volume of thermoelectric material, height, and width of the thermoelectric elements, total contact area with the heat source, total volume of the conductive metal, as illustrated in figure 6(b) and (c). Each of these three thermoelectric modules contains varying thermocouple pairs: 8, 4, and 2, respectively.

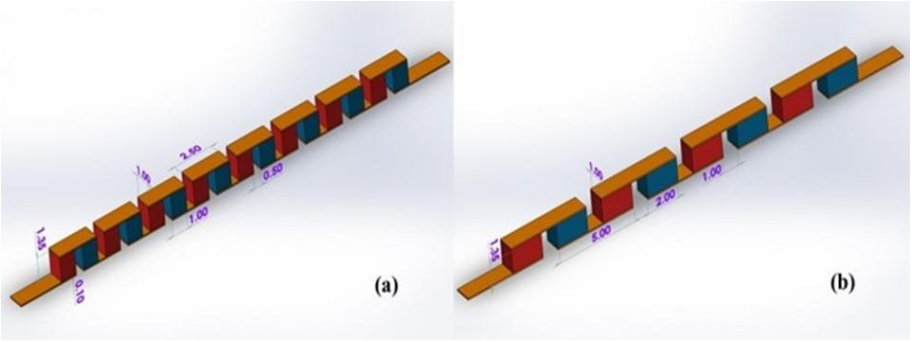

 doi:10.20944/preprints202409.1792.v

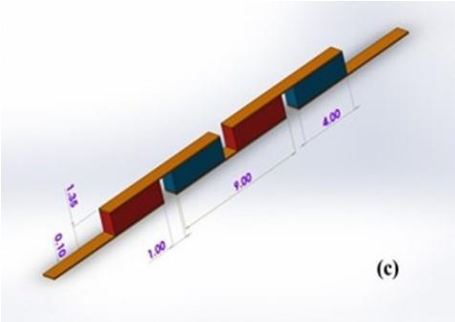

Figure 6. Structure of the Flat-Plate Thermoelectric Module with a Single Row of Thermocouples – (a) Thermoelectric Element Dimension: 1x1x1.35mm, (b) Thermoelectric Element Dimension: 2x1x1.35mm, (c) Thermoelectric Element Dimension: 4x1x1.35mm. [30].

3. Boundary Conditions and Governing Equations

In order to conduct a more in-depth investigation of the produced modules, simulations are performed using COMSOL 5.5 with the finite element analysis technique. The resolution of the governing equations encompasses various fundamental assumptions:

- The simulation experiments are carried out in a state of equilibrium.
- Thermal transfer in the thermoelectric elements occurs radially, with the lateral components being thermally isolated. Therefore, thermal radiation and Thomson effects are disregarded.
- The thermal and electrical properties of thermoelectric materials exhibit temperature-independent behavior.
- According to the maximum power transfer theorem, the thermoelectric module produces the most significant output power when the external resistance equals the internal resistance.
- The electrical and thermal contact resistances and the welding layer's resistance are not considered.

The electrical resistance within the flat-plate thermoelectric module can be calculated using the following governing equation [32]:

$$R_{pn} = \frac{\rho_p H_p}{A_p} + \frac{\rho_n H_n}{A_n} \tag{1}$$

$$R_C = \frac{\rho_C L_C}{A_C} \tag{2}$$

$$R_{TEG} = N_1 R_{pn} + N_2 R_C \tag{3}$$

In the above equations, R_{pn} represents the sum of the internal electrical resistances of the thermocouples. ρ_p is the resistivity of the p-type thermoelectric element, H_p is the height of the p-type thermoelectric element, and A_p is the heat-receiving cross-sectional area of the p-type thermoelectric element. Similarly, ϱn is the resistivity of the n-type thermoelectric element, H_n is its height, and An is its heat-receiving cross-sectional area. R_C is the internal resistance of the conductive copper strip, ρ_c is the resistivity of the copper strip, L_c is the length of the copper strip, and A_c is the cross-sectional area of the copper strip through which the current flows. R_{TEG} is the total internal resistance of the FTEG module. N_1 is the number of thermocouple pairs, and N_2 is the number of connecting copper strips.

For calculating the internal resistance of the ATEG, the following governing equation can be used [31]:

 doi:10.20944/preprints202409.1792.v

$$R_{pn} = R_p + R_n = \frac{(\rho_p+\rho_n)ln\left(\frac{r_2}{r_1}\right)}{\Delta\theta W} \tag{4}$$

$$R_C = \rho_C \frac{L_C}{A_C} \tag{5}$$

$$R_{TEG} = N_3 R_{pn} + \rho_c \left(N_4 \frac{L_{CI}}{A_I} + N_5 \frac{L_{CO}}{A_O} + N_6 \frac{L_{CC}}{A_C}\right) \tag{6}$$

In the equations, Rpn represents the sum of the resistances of the thermocouples. R_p, R_n, and R_C are the resistances of the p-type and n-type thermoelectric elements and the connecting copper strip, respectively. ρ_p、ρ_n、ρ_c are the resistivities of the p-type and n-type thermoelectric elements and the connecting copper strip, respectively. W is the width of the thermoelectric element, and Δθ is the angle of the annular thermoelectric element. r_1 and r_2 represent the inner and outer radii of the thermoelectric element, respectively. L_C denotes the length of the connecting copper strip, and L_{CI}, L_{CO}, and L_{CC} represent the inner circle, outer circle, and front and rear ring connecting copper strips of the thermoelectric element, respectively. A_c is the cross-sectional area of the copper strip through which the current flows. N_3 is the number of thermocouple pairs, and N_4、N_5、N_6 are the numbers of inner, outer, and front and rear connecting copper strips, respectively. RTEG is the total internal resistance of the annular thermoelectric module.

For calculating the maximum output power when the load resistance equals the internal resistance of the thermoelectric module, the following governing equation can be used [32]:

$$P_{max} = \frac{V_{OC}^2}{4R_{TEG}} \tag{7}$$

In the above equation, Pmax represents the maximum output power, V_{OC} is the open-circuit voltage, and R_{TEG} is the total internal resistance of the thermoelectric module.

When there is a change in the load resistance, the calculation of the output power can be determined using the following governing equation [21]:

$$V = I \times (R_L + R_{TEG}) \tag{8}$$

$$P = I^2 \times R_L \tag{9}$$

In the equation mentioned above, I represents the circuit current, R_L is the load resistance, and P is the power generated by the thermoelectric module.

The thermal efficiency of the thermoelectric module can be calculated using the following governing equation [30]:

$$\dot{Q}_h = N\left[\alpha \frac{\alpha(T_h-T_c)}{\frac{R_L}{N}+R_{TEG}} T_h - \frac{1}{2}\left[\frac{\alpha(T_h-T_c)}{\frac{R_L}{N}+R_{TEG}}\right]^2 R_{TEG} + \kappa_{TEG}(T_h - T_C)\right] \tag{10}$$

$$\dot{Q}_c = N\left[\alpha \frac{\alpha(T_h-T_c)}{\frac{R_L}{N}+R_{TEG}} T_c + \frac{1}{2}\left[\frac{\alpha(T_h-T_c)}{\frac{R_L}{N}+R_{TEG}}\right]^2 R_{TEG} + \kappa_{TEG}(T_h - T_C)\right] \tag{11}$$

$$\eta_{TEG} = \frac{P_{out}}{\dot{Q}_h} \tag{12}$$

In the aforementioned governing equation, $\dot{Q}_h$ represents the heat input at the hot end of the tubular thermoelectric generator (TTEG) and $\dot{Q}_c$ represent the heat output at the cold end of the TTEG. Both$\dot{Q}_h$ and $\dot{Q}_c$ are measured in watts (W). N denotes the number of thermoelectric elements, α is the Seebeck coefficient, T_h and T_c are the average temperatures at the hot and cold ends of the thermoelectric module, respectively. R_{TEG} and R_L respectively represent the internal resistance of the thermoelectric module and the resistance of the connected external load. κ_{TEG} is the thermal conductivity of the thermoelectric element. In the formulas for calculating the thermal energy at the

 doi:10.20944/preprints202409.1792.v

cold and hot ends, $\frac{\alpha(T_h-T_c)}{\frac{R_L}{N}+R_{TEG}}$, as stated by Faisal Albatati et al. [28], this can be replaced by the current value.

4. Results and Discussion

According to the test data provided by the manufacturer of the TGM1-127-1.0-0.8 thermoelectric module, the FTEG reached a peak power output of 5.1W when the hot-end temperature was 200°C and the cold-end temperature was 30°C. Subsequently, we performed simulated studies on the FTEG depicted in Figure 1 and the ATEG displayed in Figure 3(a), utilizing identical thermoelectric material volume and the testing circumstances specified by the manufacturer. The findings demonstrated that when subjected to an identical temperature differential between the hot and cold sections, the FTEG produced an open-circuit voltage of 13.42V and an output power of 5.81W. This output power is 1.14 times higher than the test data provided by the manufacturer. Similarly, in the case of the simulated ATEG, when the hot-end temperature was set to 200°C and the cold-end temperature was set to 30°C, it generated an open-circuit voltage of 11.36V and produced an output power of 9.43W. This represents a 3.62W increase, corresponding to a 62.34% rise compared to the FTEG.

4.1. Validation of Single Thermocouple Output Performance

In order to assess the thermoelectric power generation capabilities of the ATEG, a first simulation experiment was carried out on a single annular thermocouple located within the ATEG module. We examined three groups of thermocouples, each with the same height but varying volumes of thermoelectric material and heat-receiving cross-sectional areas. These differences are illustrated in Figures 3(d), 4(b), and 5(b), where the volumes and areas are 1, 2, and 4 times bigger, respectively. During these simulations, the lower temperature limit was set at 30°C, while the upper temperature limit ranged from 100°C to 250°C in increments of 10°C. Figures 7 and 8 depict the open-circuit voltage and output power produced by these thermocouples in response to variations in temperature. Figure 7 shows that the three sets of thermocouples produce nearly identical open-circuit voltage values when subjected to the same temperature difference. This suggests that increasing the size and heat-receiving area of the thermocouples does not result in a higher open-circuit voltage. Figure 8 demonstrates that augmenting the volume of thermoelectric material results in a proportional rise in current, thereby amplifying the output power.

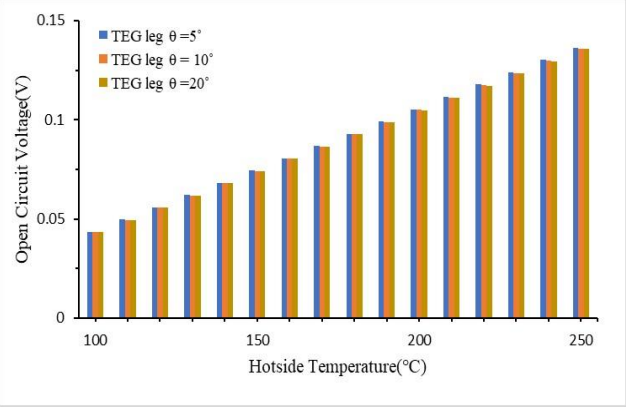

Figure 7. Open-circuit voltage values for annular thermocouples with varying volumes of thermoelectric material and heat-receiving cross-sectional areas at different temperatures.[30].

 doi:10.20944/preprints202409.1792.v

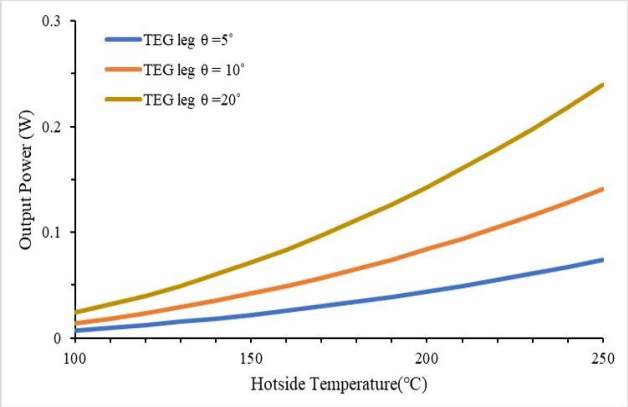

Figure 8. Output power values for annular thermocouples with varying volumes of thermoelectric material at different temperatures.[30].

In order to validate the fundamental thermoelectric performance of individual square thermocouples in the FTEG module, we examined three groups of thermocouples depicted in Figures 6(a), (b), and (c). These thermocouples have the same height, but their volumes of thermoelectric material and heat-receiving cross-sectional areas are 1, 2, and 4 times larger, respectively. The simulations maintained a constant cold-end temperature of 30°C, whereas the hot-end temperature varied at 10°C intervals between 100°C and 250°C. The fluctuations in the open-circuit voltage (Figure 9) and output power (Figure 10) produced by these thermocouples were comparable to those witnessed in the annular thermocouples. Hence, the outcomes of the individual thermocouple simulation trials for both annular and square thermocouples align with the findings reported in the scholarly works of Pan Wang et al. [27] and Yongming Shi et al. [28].

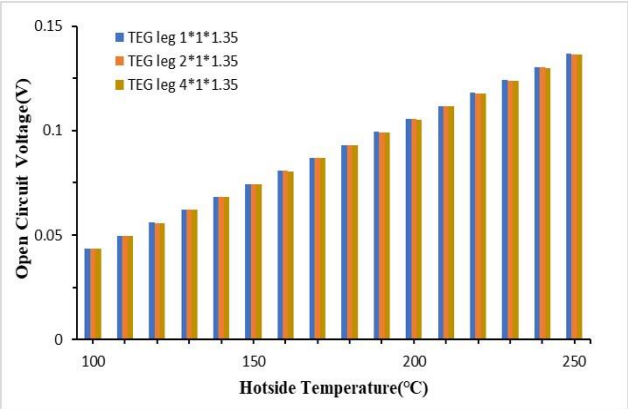

Figure 9. Open-circuit voltage values for rectangular thermocouples with varying volumes of thermoelectric material and heat-receiving cross-sectional areas at different temperatures.[30].

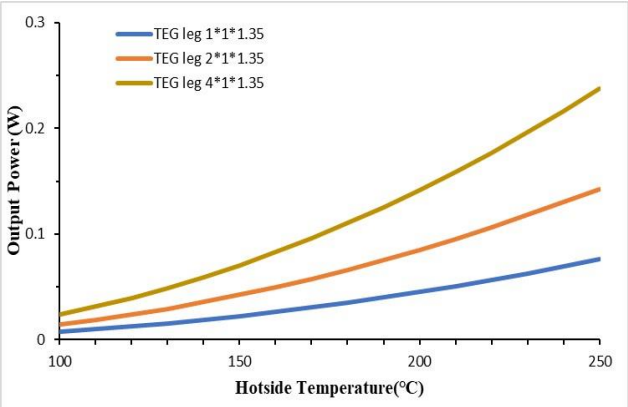

 doi:10.20944/preprints202409.1792.v

Figure 10. Output power values for rectangular thermocouples with varying volumes of thermoelectric material at different temperatures.[30].

4.2. Impact of Thermocouple Quantity on ATEG Output Performance

To understand the influence of the varying number of thermoelectric elements within the ATEG on its thermoelectric output performance (including open-circuit voltage, current, output power, and thermal efficiency), we analyzed three sets of ATEG modules. These modules, depicted in Figures 3(c), 4(a), and 5(a), have the same total volume of thermoelectric material and connecting copper plates, total heat-receiving area, shape, and height of the thermoelectric elements. The experiments were conducted with the hot-end temperature varying in 10°C increments from 100°C to 250°C while maintaining the cold-end temperature constant at 30°C. Figure 11 shows the open-circuit voltage values of the three different sets of ATEG under various hot-end temperatures. It was observed, as mentioned in many literatures, that at the same volume of thermoelectric material, the thermoelectric module with a smaller angle (5°) between elements, and hence a higher number of thermocouples in series, achieves a higher open-circuit voltage, with the number of thermoelectric elements and open-circuit voltage being directly proportional. Figure 12 presents the current values when the three sets of ATEG generate maximum power output with the external load equal to the internal load of the TEG under different hot-end temperatures. It can be noted that ATEGs with fewer internal thermoelectric elements, although generating lower open-circuit voltages, can produce higher current values due to their larger volume of thermoelectric elements.

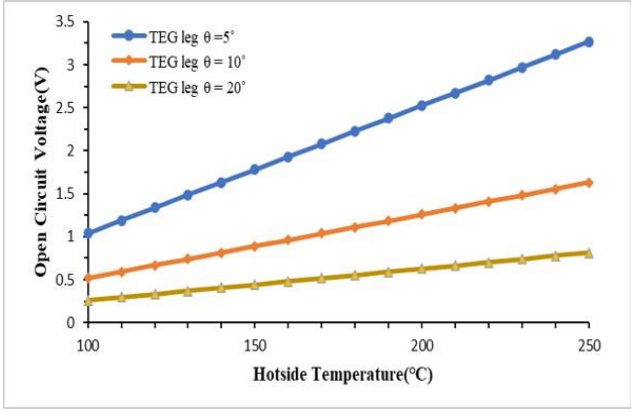

Figure 11. Open-circuit voltage values of ATEG under different temperature differences and numbers of thermoelectric couples.[30].

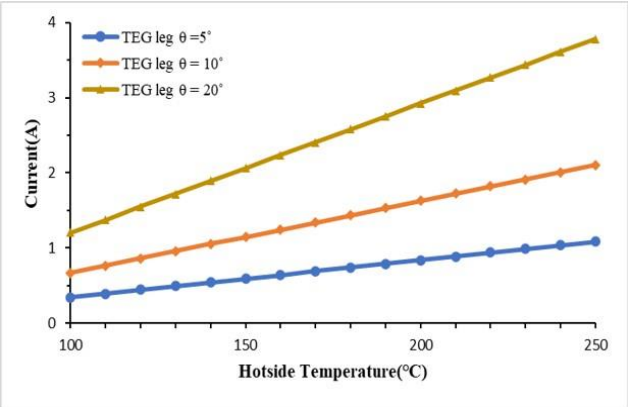

Figure 12. Current values of ATEG under different temperature differences and numbers of thermoelectric couples.[30].

Figure 13 displays the highest achievable power output values of three sets of ATEGs with varying quantities of thermoelectric elements at different hot-end temperatures. The graph

 doi:10.20944/preprints202409.1792.v

demonstrates that the open-circuit voltage of the ATEG is at its peak when the angle between the thermoelectric elements is 5°, allowing for the most significant number of elements within the module. Despite being smaller in this configuration, it attains the most output power under identical heat-receiving conditions. Figure 14 illustrates the thermal efficiency at the maximum output power values for the three sets of ATEGs at varying hot-end temperatures. When comparing Figure 13 to the other scenarios, it is evident that despite having the same total heat-receiving area and identical height and shape of the thermoelectric elements, the ATEG with a 5° angle between elements generates the highest output power but exhibits the lowest thermal efficiency.

In contrast, the ATEG with a 20° angle between components has the maximum thermal efficiency while simultaneously having the lowest output power. The main reason is the reduced quantity of thermocouples and the increased output current in the 20° configuration. The magnitude of the output current of the thermoelectric module is also contingent upon the volume of the thermoelectric elements. Hence, when considering the thermoelectric material within the module under identical volume conditions, the quantity of thermoelectric elements becomes a crucial aspect in augmenting the output power.

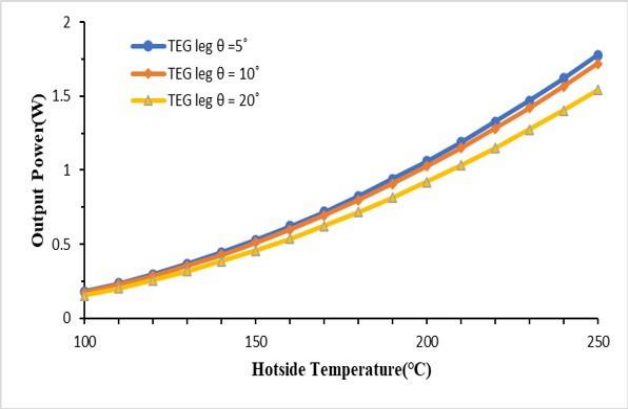

Figure 13. Maximum output power values for ATEG with different angles between thermoelectric elements at varying hot-end temperatures.[30].

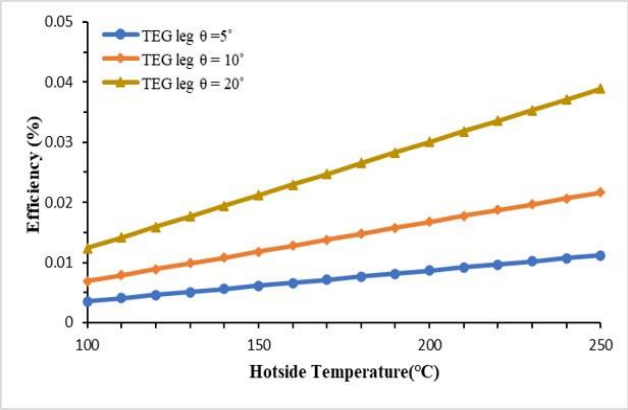

Figure 14. Thermal efficiency values for ATEG with different angles between thermoelectric elements at varying hot-end temperatures.[30].

By utilizing the ATEG with a 20° angle per annular thermoelectric element as a reference point, an examination of Figure 15 demonstrates that the output power values of the three sets of thermoelectric modules, with element angles of 20°, 10°, and 5°, increase proportionally as the hot-end temperature rises. This ratio remains consistent. The module with a 5° angle exhibits a fixed proportion increase in output power compared to the 20° angle, amounting to 15.19%. Likewise, the rise in the module with a 10° angle relative to the 20° module is also a constant number, maintaining

 doi:10.20944/preprints202409.1792.v

a ratio of 11.41%. The observed increase in the output power of the thermoelectric modules is due to the alteration in the number of thermocouples included in the ATEG.

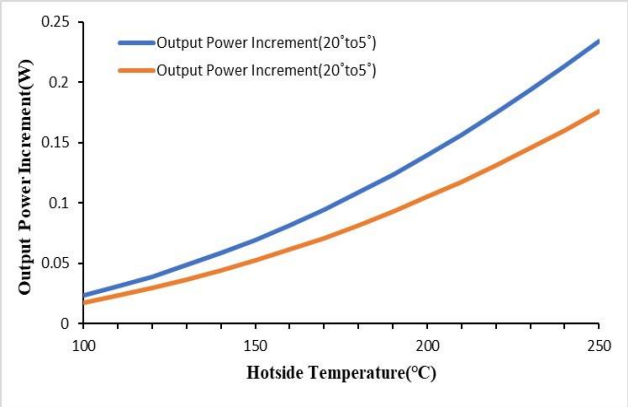

Figure 15. Comparison of ATEG output power with different numbers of thermocouples.[30].

Figure 16 illustrates the correlation between the output power of ATEGs and the changes in external load resistance. The cold-end temperature remains constant at 30°C, while the hot-end temperatures are fixed at 100°C, 150°C, 200°C, and 250°C. The analysis demonstrates that in ATEGs, including varying quantities of internal thermocouples, a rise in the hot-end temperature exclusively augments the ATEG's output power. Nevertheless, the correlation between the output powers of these three sets of ATEGs remains unaffected by an increase in load resistance. The number of thermocouples within the ATEG does not affect the change in output power when modifying the external load resistance, even under different temperature differential situations.

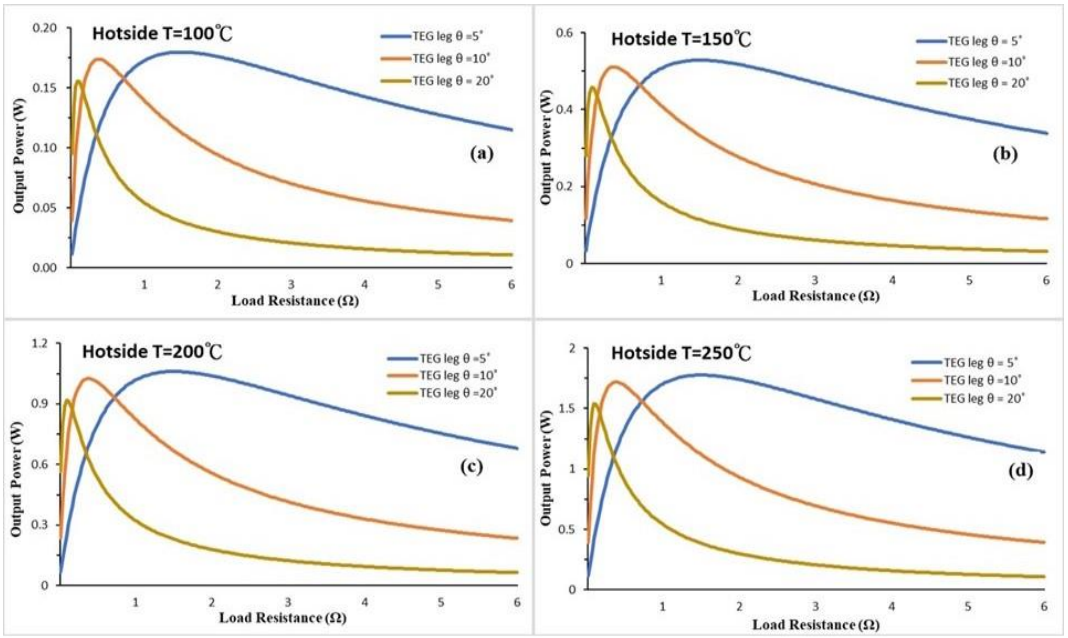

Figure 16. Relationship between ATEG output power and load: (a) hot side temperature 100℃, (b) hot side temperature 150℃, (c) hot side temperature 200℃, (d) hot side temperature 250℃.[30].

4.3. Impact of Thermocouple Quantity on FTEG Output Performance

Our study focused on the FTEG and tried to validate and comprehend whether the correlation between the number of thermoelectric components and output power is exclusive to ATEGs or applies to other structural configurations of thermoelectric modules. We conducted simulations on three sets of thermoelectric modules, each with the same volume of thermoelectric material but with varied dimensions. These dimensions are illustrated in Figure 6: (a) 1x1x1.35 mm, (b) 2x1x1.35 mm,

 doi:10.20944/preprints202409.1792.v

and (c) 4x1x1.35 mm. The experiments were conducted using identical settings, where the hot-end temperature varied from 100°C to 250°C in increments of 10°C, while the cold-end temperature remained constant at 30°C. Figures 17 and 18 display the open-circuit voltage and current values obtained when the three sets of FTEG, each with varying numbers of thermoelectric elements, are subjected to varied hot-end temperatures. These values correspond to the maximum power output. When the dimension of the thermoelectric element is 1x1x1.35 mm, the FTEG exhibits the most number of thermoelectric elements, leading to the highest output voltage but the lowest current value. This observation aligns with the findings obtained from ATEG simulations.

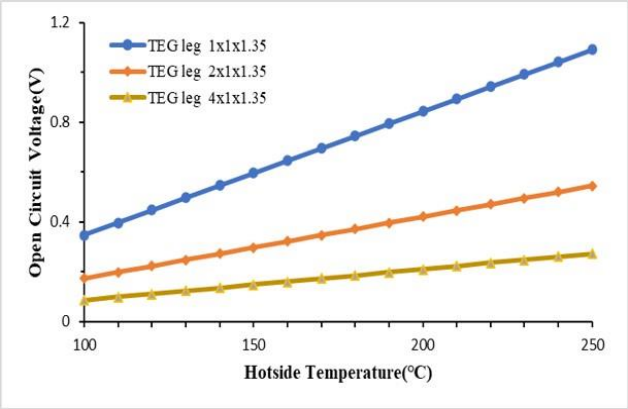

Figure 17. Open-circuit voltage values for FTEG with different thermoelectric element dimensions at varying hot-end temperatures.[30].

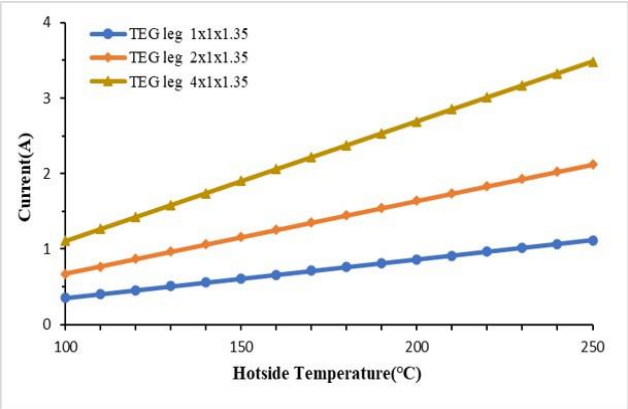

Figure 18. Current values for FTEG with different thermoelectric element dimensions at varying hot-end temperatures.[30].

Figures 19 and 20 display the highest power output values and thermal efficiency for the three sets of FTEGs with varying sizes of thermoelectric elements at varied hot-end temperatures. Upon analyzing the simulation results, it is evident that increasing the number of thermoelectric elements within the module leads to a more considerable output power. This is observed when the thermoelectric element size is set at 1x1x1.35 mm. Nevertheless, at the peak output power of the thermoelectric module, the thermal efficiency decreases due to the increased quantity of thermoelectric elements. In contrast, when the dimension of the thermoelectric element is 4x1x1.35 mm, reducing the number of thermoelectric components in the module results in decreased output power but increased thermal efficiency. The conclusions obtained from the ATEG simulation experiments in Figures 9 and 10 are consistent with the results of the simulations.

 doi:10.20944/preprints202409.1792.v

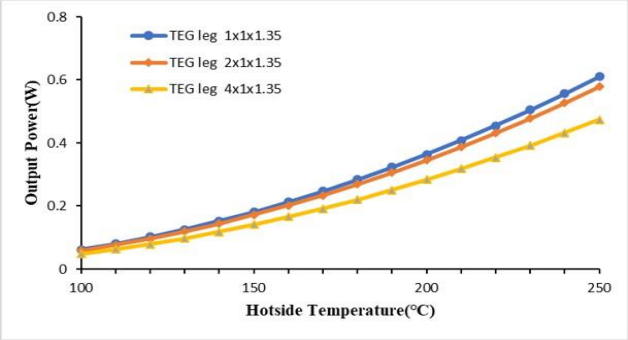

Figure 19. Maximum output power values for FTEG with different thermoelectric element dimensions at varying hot-end temperatures.[30].

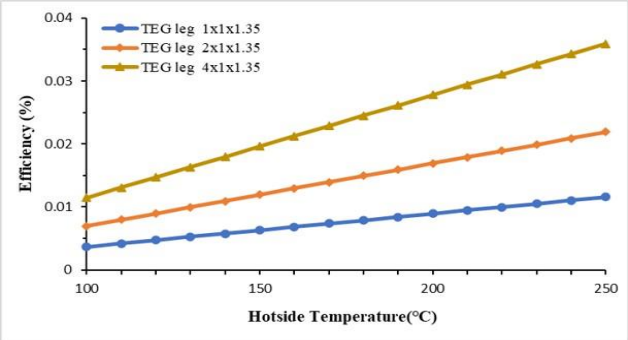

Figure 20. Thermal efficiency values for FTEG with different thermoelectric element dimensions at varying hot-end temperatures.[30].

Figure 21 depicts a comparative graph that illustrates the size of the thermoelectric element, which measures 4x1x1.35 mm. The graph illustrates that the output power of the three sets of thermoelectric modules, with element sizes of 4x1x1.35 mm, 2x1x1.35 mm, and 1x1x1.35 mm, grows proportionally as the hot-end temperature rises. Furthermore, the rate of increase remains constant. The module with a 1x1x1.35 mm element size has an output power of 28.53% greater than that with a 4x1x1.35 mm element size. Similarly, the module with a 2x1x1.35 mm element size has an output power of 21.77% higher than the 4x1x1.35 mm module. The main reason for the rise in output power is the alteration in the quantity of thermocouples included in the FTEG. Hence, the quantity of thermoelectric components is a determining factor that influences the power generated in ATEG and has a comparable effect on FTEG.

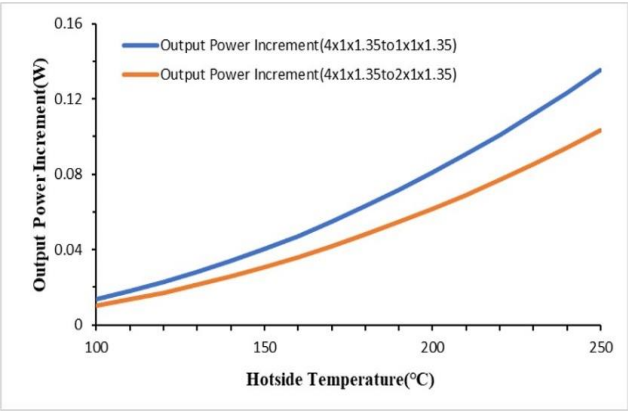

Figure 21. Output power values for FTEG with different thermoelectric element dimensions at varying hot-end temperatures.[30].

 doi:10.20944/preprints202409.1792.v

Figure 22 depicts a graph that demonstrates the correlation between the output power of FTEG and the change in load resistance. The cold-end temperature is held constant at 30°C, while the hot-end temperatures are adjusted to 100°C, 150°C, 200°C, and 250°C. For FTEGs with varying numbers of thermocouples, a rise in the hot-end temperature results in a corresponding increase in the output power. Nevertheless, the variation in the number of thermocouples present in the FTEG does not impact this observed rise. The output powers of FTEGs with different numbers of thermocouples stay constant regardless of variations in hot-end temperature.

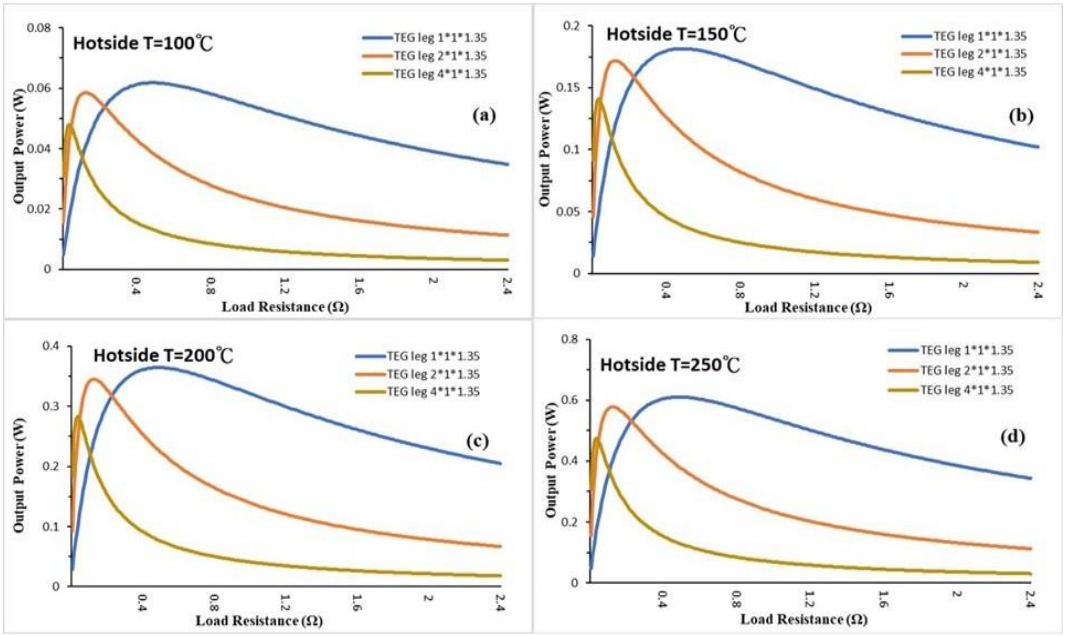

Figure 22. Output power values for FTEG at different hot-end temperatures and varying load resistance: (a) hot side temperature 100℃, (b) hot side temperature 150℃, (c) hot side temperature 200℃, (d) hot side temperature 250℃.[30].

Based on the previous explanations, it is clear that in both ATEG and FTEG modules, the size of the thermoelectric elements, the contact area with the heat source, and the volume of the conductive metal all play a role in addition to the total volumFe of thermoelectric material. Furthermore, the number of thermoelectric elements not only determines the open-circuit voltage but also significantly impacts the output power of the thermoelectric module.

5. Conclusions

In many studies, it has been found that the shape and height of thermoelectric elements, the contact area with the heat source, the heating temperature, and the volume of the connecting copper plate are all factors affecting output power. After eliminating these influencing factors, this study changed only the number of thermoelectric couples within the thermoelectric module and reached the following conclusions:

1. Different numbers of thermoelectric couples within the thermoelectric module do not affect the trend of thermoelectric output performance.
2. The number of thermoelectric elements determines not only the level of the open-circuit voltage of the thermoelectric module but also affects the amount of output power.
3. Under the same total volume of thermoelectric material, thermoelectric element height, total contact area with the heat source, total volume of connecting copper plate, and heating conditions, there is a proportional increase in output power with different numbers of thermoelectric couples in the module.
4. For thermoelectric modules with different numbers of thermoelectric couples, the trend of

 doi:10.20944/preprints202409.1792.v

output power change due to load resistance variation does not differ with changes in the temperature difference of heating.

5. The above phenomena exist not only in ATEG (Automotive Thermoelectric Generator) but also in FTEG (Flexible Thermoelectric Generator).

Author Contributions: Conceptualization, C.-I W. and K.-W. D.; methodology, C.-I W. and K.-W. D.; software, K.-W. D. and Y.-H. T.; validation, K.-W. D. and Y.-H. T.; formal analysis, C.-I W. and K.-W. D.; investigation, C.-I W. and K.-W. D.; resources, C.-I W.; data curation, K.-W. D. and Y.-H. T.; writing—original draft preparation, C.-I W. and K.-W. D.; writing—review and editing, C.-I W.; visualization, K.-W. D. and Y.-H. T.; supervision, C.-I W.; project administration, C.-I W.; funding acquisition, C.-I W.. All authors have read and agreed to the published version of the manuscript.

Funding: This research was funded by National Science and Technology Council of Taiwan, grant number 111-2221-E-019-060-.

Data Availability Statement: Data can be obtained by contacting the author, Chun-I Wu (wuchuni@ntou.edu.tw).

Acknowledgments: The authors would like to thank the reviewers for their comments on improving the quality of the paper.

Conflicts of Interest: The authors declare no conflicts of interest.

References

1. Jouhara, H.; Żabnieńska-Góra, A.; Khordehgah, N.; Doraghi, Q.; Ahmad, L.; Norman, L.; Axcell, B.; Wrobel, L.; Dai, S. Thermoelectric generator (TEG) technologies and applications. *International Journal of Thermofluids* **2021**, *9*, 100063.
2. Zoui, M.A.; Bentouba, S.; Stocholm, J.G.; Bourouis, M. A review on thermoelectric generators: Progress and applications. *Energies* **2020**, *13*, 3606.
3. Dai, D.; Zhou, Y.; Liu, J. Liquid metal based thermoelectric generation system for waste heat recovery. *Renewable Energy* **2011**, *36*, 3530-3536.
4. DHINGRA, A.; KUMAR, D.; SAINI, V. Thermo Electric Generator. *IRE Journals* **2018**, *1*, doi:1700652.
5. Shittu, S.; Li, G.; Zhao, X.; Ma, X. Review of thermoelectric geometry and structure optimization for performance enhancement. *Applied Energy* **2020**, *268*, 115075.
6. Huang, S.; Xu, X. A regenerative concept for thermoelectric power generation. *Applied Energy* **2017**, *185*, 119-125.
7. Thimont, Y.; LeBlanc, S. The impact of thermoelectric leg geometries on thermal resistance and power output. *Journal of Applied Physics* **2019**, *126*.
8. Zhou, X.; Yan, Y.; Lu, X.; Zhu, H.; Han, X.; Chen, G.; Ren, Z. Routes for high-performance thermoelectric materials. *Materials Today* **2018**, *21*, 974-988.
9. Shen, Z.-G.; Liu, X.; Chen, S.; Wu, S.-Y.; Xiao, L.; Chen, Z.-X. Theoretical analysis on a segmented annular thermoelectric generator. *Energy* **2018**, *157*, 297-313.
10. We, J.H.; Kim, S.J.; Cho, B.J. Hybrid composite of screen-printed inorganic thermoelectric film and organic conducting polymer for flexible thermoelectric power generator. *Energy* **2014**, *73*, 506-512.
11. Zhang, A.; Wang, B.; Pang, D.; Chen, J.B.; Wang, J.; Du, J. Influence of leg geometry configuration and contact resistance on the performance of annular thermoelectric generators. *Energy Conversion and Management* **2018**, *166*, 337-342.
12. Zhu, W.; Weng, Z.; Li, Y.; Zhang, L.; Zhao, B.; Xie, C.; Shi, Y.; Huang, L.; Yan, Y. Theoretical analysis of shape factor on performance of annular thermoelectric generators under different thermal boundary conditions. *Energy* **2022**, *239*, 122285.
13. Wang, S.; Xie, T.; Xie, H. Experimental study of the effects of the thermal contact resistance on the performance of thermoelectric generator. *Applied Thermal Engineering* **2018**, *130*, 847-853.
14. Sakamoto, T.; Iida, T.; Sekiguchi, T.; Taguchi, Y.; Hirayama, N.; Nishio, K.; Takanashi, Y. Selection and evaluation of thermal interface materials for reduction of the thermal contact resistance of thermoelectric generators. *Journal of electronic materials* **2014**, *43*, 3792-3800.
15. Bjørk, R.; Christensen, D.V.; Eriksen, D.; Pryds, N. Analysis of the internal heat losses in a thermoelectric generator. *International Journal of Thermal Sciences* **2014**, *85*, 12-20.
16. Narjis, A.; Liang, C.-T.; El Aakib, H.; Tchenka, A.; Outzourhit, A. Design optimization for maximized thermoelectric generator performance. *Journal of Electronic Materials* **2020**, *49*, 306-310.

 doi:10.20944/preprints202409.1792.v

17. Brito, F.; Figueiredo, L.; Rocha, L.; Cruz, A.; Goncalves, L.; Martins, J.; Hall, M. Analysis of the effect of module thickness reduction on thermoelectric generator output. *Journal of Electronic Materials* **2016**, *45*, 1711-1729.
18. Ming, T.; Yang, W.; Huang, X.; Wu, Y.; Li, X.; Liu, J. Analytical and numerical investigation on a new compact thermoelectric generator. *Energy Conversion and Management* **2017**, *132*, 261-271.
19. Wang, L.; Li, K.; Zhang, S.; Liu, C.; Zhang, Z.; Chen, J.; Gu, M. Modeling the effects of module size and material property on thermoelectric generator power. *ACS omega* **2020**, *5*, 29844-29853.
20. Fan, S.; Gao, Y. Numerical simulation on thermoelectric and mechanical performance of annular thermoelectric generator. *Energy* **2018**, *150*, 38-48.
21. Zhang, M.; Wang, J.; Tian, Y.; Zhou, Y.; Zhang, J.; Xie, H.; Wu, Z.; Li, W.; Wang, Y. Performance comparison of annular and flat-plate thermoelectric generators for cylindrical hot source. *Energy Reports* **2021**, *7*, 413-420.
22. Wang, J.; Li, Y.; Zhao, C.; Cai, Y.; Zhu, L.; Zhang, C.; Wang, J.; Zhao, W.; Cao, P. An optimization study of structural size of parameterized thermoelectric generator module on performance. *Energy Conversion and Management* **2018**, *160*, 176-181.
23. Manikandan, S.; Kaushik, S. Energy and exergy analysis of solar heat pipe based annular thermoelectric generator system. *Solar Energy* **2016**, *135*, 569-577.
24. Elsabahy, M.M.; Rabie, R.; Ahmed, M. Performance study of thermoelectric power generators at different geometrical configurations. In Proceedings of the Energy Sustainability, 2021; p. V001T005A004.
25. Meng, F.; Chen, L.; Sun, F. Effects of thermocouples' physical size on the performance of the TEG–TEH system. *International Journal of Low-Carbon Technologies* **2016**, *11*, 375-382.
26. Fan, L.; Zhang, G.; Wang, R.; Jiao, K. A comprehensive and time-efficient model for determination of thermoelectric generator length and cross-section area. *Energy Conversion and Management* **2016**, *122*, 85-94.
27. Wang, P.; Wang, B.; Wang, K.; Gao, R.; Xi, L. An analytical model for performance prediction and optimization of thermoelectric generators with varied leg cross-sections. *International Journal of Heat and Mass Transfer* **2021**, *174*, 121292.
28. Shi, Y.; Zhu, Z.; Deng, Y.; Zhu, W.; Chen, X.; Zhao, Y. A real-sized three-dimensional numerical model of thermoelectric generators at a given thermal input and matched load resistance. *Energy Conversion and Management* **2015**, *101*, 713-720.
29. Albatati, F.; Attar, A. Analytical and experimental study of thermoelectric generator (TEG) system for automotive exhaust waste heat recovery. *Energies* **2021**, *14*, 204.
30. Du, K.-W. Modeling of Thermoelectric Generator and Cooling System. National Taiwan Ocean University, Taiwan, 2024.
31. Tian, X.-X.; Asaadi, S.; Moria, H.; Kaood, A.; Pourhedayat, S.; Jermsittiparsert, K. Proposing tube-bundle arrangement of tubular thermoelectric module as a novel air cooler. *Energy* **2020**, *208*, 118428.
32. Quan, R.; Liu, G.; Wang, C.; Zhou, W.; Huang, L.; Deng, Y. Performance investigation of an exhaust thermoelectric generator for military SUV application. *Coatings* **2018**, *8*, 45.